Galvano-magnetic and magneto-optical properties of transition metal systems

H. Ebert [a], **G.-Y. Guo** [b] and **J. Banhart** [c]

[a] Inst. f. Phys. Chemie der Univ., Theresienstr. 37, D-80333 München

[b] EPSRC Daresbury Laboratory, Warrington WA4 4AD, UK

[c] Fraunhofer-Institut for Applied Materials Research, Lesumer Heerstr. 36, D-28717 Bremen

The abstracts collected in the last issues of this newsletter are a nice demonstration that within the *Network Community* there is considerable interest in the impact of relativistic effects on the electronic structure. Obviously, spin-orbit coupling plays a prominent role in magnetic solids because on one hand it gives rise to a large number of interesting phenomena and on the other it poses a big challenge to the basic formalism as well as implementation. The latter is caused by the demand that both spin-orbit coupling and magnetism have to be accounted for at the same time. The most advanced Hamiltonian, commonly used today, which meets this requirement is briefly described here. It is demonstrated for the conductivity tensor how simple symmetry considerations allow to predict the consequences of the interplay between spin-orbit coupling and magnetism. Recent calculations for the DC conductivity, Kerr-rotation and magnetic X-ray dichroism for various transition metal systems indicate that the above mentioned Hamiltonian supplies a sound basis for understanding all these phenomena giving (in general) a quantitative description of them.

3 Dirac Hamiltonian and band structure schemes

As already pointed out in 1973 by Rajagopal and Callaway, treating magnetism in a proper relativistic way, by extending the original Hohenberg-Kohn-Sham density formalism, leads to a current density formalism with the expectation value of the four-current density operator as the central quantity. Unfortunately, this approach seems to be – at least for the moment – too ambitious. Therefore, in order to describe relativistic effects and spontanous magnetism on an equal footing one has to use an extension of the non-relativistic spin-density-functional formalism in the form originally suggested by McDonald and Vosko [1]. The corresponding Dirac-Hamiltonian has the form:

$$\mathcal{H}_D = \frac{c}{i}\boldsymbol{\alpha}\cdot\boldsymbol{\nabla} + \frac{1}{2}(\beta - I) + V_H(\mathbf{r}) + \bar{V}_{xc}(\mathbf{r}) + V_{spin}(\mathbf{r}), \qquad (1)$$

with α_i and β being the standard Dirac matrices and $V_H(\mathbf{r})$ the Hartree potential. The exchange correlation potential consists of a spin averaged- and a spin-dependent part, with

the latter given by:

$$V_{spin}(\mathbf{r}) = \beta\boldsymbol{\sigma} \cdot \frac{\partial E_{xc}}{\partial \mathbf{m}}(\mathbf{r}) = \beta\boldsymbol{\sigma} \cdot \mathbf{B}(\mathbf{r}), \tag{2}$$

where $\mathbf{m}$ is the spin magnetisation density. Obviously, any explicit coupling to the orbital degree of freedom of the electrons is ignored in the potential terms of the above Hamiltonian, but it would be present in the framework of a more general current density functional formalism.

As demonstrated by Feder et al. [2] and Strange et al. [3], when dealing with an isolated spherically symmetric potential well (i.e. $V(\mathbf{r}) = V(r)$ and $\mathbf{B}(\mathbf{r}) = \mathbf{B}(r)$) the most important consequence of $V_{spin}(\mathbf{r})$ is that the solutions $\Psi_\Lambda(\mathbf{r}, E)$ of the above Hamiltonian have in general no unique spin angular character. Fortunately, the summation in

$$\Psi_\Lambda(\mathbf{r}, E) = \sum_{\Lambda'} \Psi_{\Lambda'\Lambda}(\mathbf{r}, E) = \sum_{\Lambda'} \begin{pmatrix} g_{\Lambda'\Lambda}(r, E)\, \chi_{\Lambda'}(\hat{\mathbf{r}}) \\ i f_{\Lambda'\Lambda}(r, E)\, \chi_{-\Lambda'}(\hat{\mathbf{r}}) \end{pmatrix}, \tag{3}$$

where $\chi_\Lambda(\hat{\mathbf{r}})$ are the spin-angular functions and $\pm\Lambda = (\pm\kappa, \mu)$ are relativistic quantum numbers, is restricted to $\mu' = \mu$ and $\kappa' = \kappa, -\kappa - 1$ (i.e. $p_{1/2,\mu} - p_{3/2,\mu}, d_{3/2,\mu} - d_{5/2,\mu}, \ldots$), which seems to be sufficient for all interesting cases.

Starting from $\Psi_\Lambda(\mathbf{r}, E)$ as the solution of the single site problem spin polarized relativistic (SPR) versions of the LMTO- and KKR-methods have been developed by various groups.

4 Symmetry considerations

A direct consequence of the Hamiltonian in Eq. (1) is that the symmetry of a system depends on the direction $\hat{\mathbf{M}}$ of its magnetisation $\mathbf{M}$ or equivalently on the direction of the effective magnetic field $\mathbf{B}$ in Eq. (2). Obviously, this also applies to the irreducible part of the Brillouin zone that is determined by the corresponding magnetic point group. Since symmetry imposes restrictions on the form of any equilibrium property tensor, again this will depend on $\hat{\mathbf{M}}$. Symmetry restrictions on transport property tensors have been discussed by Kleiner [4] in a general way. Here it is sufficient to consider the restrictions due to the Laue group which emerges from the magnetic space group by replacing every translation by the identity and every improper rotation by its proper counterpart.

For the frequency dependent conductivity tensor $\boldsymbol{\sigma}(\omega)$ of a cubic system one gets for example for $\hat{\mathbf{M}}[001]$:

$$\boldsymbol{\sigma}(\omega) = \begin{pmatrix} \sigma_{xx} & \sigma_{xy} & 0 \\ -\sigma_{xy} & \sigma_{xx} & 0 \\ 0 & 0 & \sigma_{zz} \end{pmatrix} \tag{4}$$

and for $\hat{\mathbf{M}}[110]$

$$\boldsymbol{\sigma}(\omega) = \begin{pmatrix} \sigma_{xx} & \sigma_{xy} & \sigma_{xz} \\ \sigma_{xy} & \sigma_{xx} & -\sigma_{xy} \\ -\sigma_{xz} & \sigma_{xz} & \sigma_{zz} \end{pmatrix}. \tag{5}$$

Here one should note that the reduction in symmetry due to the magnetisation that is manifested by Eqs. (4) and (5) occurs only if spin-orbit coupling is present. If one could switch off spin-orbit coupling for a spin-polarized system its properties would not depend anymore on the orientation of the magnetisation and for this reason its symmetry would be that of the corresponding paramagnetic state. Thus it is magnetisation together with spin-orbit coupling that leads to a symmetry reduction compared to the paramagnetic case. The extent to which this reduction in symmetry takes place is determined by the orientation of the magnetisation. However, whether the spin-orbit induced property is observable or not still depends on the magnitude of the magnetisation and the strength of the spin-orbit coupling.

5 Galvano-magnetic properties of disordered alloys

The dependence of the conductivity tensor $\boldsymbol{\sigma}(\omega = 0)$ on the spontanous magnetisation $\mathbf{M}$ of a system gives rise to the so-called galvano-magnetic phenomena. According to Eq. (4) the corresponding resistivity tensor $\boldsymbol{\rho} = \boldsymbol{\sigma}^{-1}$ for a cubic system with $\hat{\mathbf{M}}[001]$ has the form:

$$\boldsymbol{\rho} = \begin{pmatrix} \rho_{\perp} & -\rho_H & 0 \\ \rho_H & \rho_{\perp} & 0 \\ 0 & 0 & \rho_{\parallel} \end{pmatrix}. \tag{6}$$

Obviously, the off-diagonal element ρ_H can be seen as a direct measure of the anomalous Hall resistivity (AHR). The so-called spontanous magneto-resistance anisotropy (SMA) on the other hand is defined as the ratio

$$\frac{\Delta\rho}{\bar{\rho}} = \frac{\rho_{\parallel} - \rho_{\perp}}{\bar{\rho}}, \tag{7}$$

with the isotropic resistivity $\bar{\rho} = 1/3\,(2\rho_{\perp} + \rho_{\parallel})$.

An adequate prescription for calculating the residual resistivity $\boldsymbol{\rho}$ of a disordered alloy system at $T = 0K$ or the corresponding conductivity $\boldsymbol{\sigma}$ is supplied by the Kubo-Greenwood-equation:

$$\sigma_{\mu\nu} = \frac{\hbar}{\pi V_{\mathsf{cryst}}} \mathrm{Tr} \left\langle j_{\mu}\, \mathrm{Im}G^{+}(E_{\mathrm{F}})\, j_{\nu}\, \mathrm{Im}G^{+}(E_{\mathrm{F}}) \right\rangle_{\mathsf{conf.}}. \tag{8}$$

Here j_{μ} is the μ-th spatial component of the electronic current density operator $\mathbf{j}$, G^{+} is the single particle Greens function at the Fermi energy E_F and $< ... >_{\mathsf{conf.}}$ denotes the atomic configuration average for a disordered alloy.

Butler [5] has worked out in detail how this expression can be evaluated within the framework of the non-relativistic KKR-CPA formalism. As we have seen above the non-isotropic form of $\boldsymbol{\sigma}$ stems from the interplay of magnetism and spin-orbit coupling. Therefore, in order to account for galvano-magnetic effects Eq. (8) has to be evaluated within a relativistic framework. Accordingly, G^+ is:

$$\begin{aligned} G^+(\mathbf{r},\mathbf{r}',E) &= \sum_{\Lambda\Lambda'} Z_\Lambda(\mathbf{r},E)\,\tau_{\Lambda\Lambda'}(E)\,Z^\times_{\Lambda'}(\mathbf{r}',E) \\ &- \sum_{\Lambda} Z_\Lambda(\mathbf{r}_<,E)\,J^\times_\Lambda(\mathbf{r}_>,E), \end{aligned} \tag{9}$$

with $\tau_{\Lambda\Lambda'}$ the scattering path operator and $Z_\Lambda\,(J_\Lambda)$ the regular (irregular) solution of the single-site Dirac equation (see Eq. (1)) normalized according to the scattering theory.

The proper relativistic form for the current density operator $\mathbf{j}$ is $ec\boldsymbol{\alpha}$. However, when using this expression in the atomic sphere approximation (ASA) the electronic wavefunction in the interstitial region may not be accurate enough. This problem can be circumvented by using one of the following transformations of the matrix elements

$$\begin{aligned} <\phi_\Lambda(E)|\boldsymbol{\alpha}\cdot\mathbf{a}_\lambda|\phi_{\Lambda'}(E')> &= \frac{2c}{c^2+E+E'} <\phi_\Lambda(E)|\,\frac{1}{i}\boldsymbol{\nabla}\cdot\mathbf{a}_\lambda \\ &\qquad +\frac{v}{c}\boldsymbol{\alpha}\cdot\mathbf{a}_\lambda - \frac{B}{c}i\beta(\boldsymbol{\alpha}\times\mathbf{a}_\lambda)_z\,|\phi_{\Lambda'}(E')> \end{aligned} \tag{10}$$

$$\begin{aligned} &= \frac{2}{(E+c^2/2)^2-(E'+c^2/2)^2} \\ &\quad\times\Big[ic <\phi_\Lambda(E)|\boldsymbol{\nabla}V\cdot\mathbf{a}_\lambda + \beta\sigma_z\boldsymbol{\nabla}B\cdot\mathbf{a}_\lambda|\phi_{\Lambda'}(E')> \\ &\qquad -(E-E') <\phi_\Lambda(E)|V\boldsymbol{\alpha}\cdot\mathbf{a}_\lambda - iB\beta\sigma_z(\boldsymbol{\alpha}\times\mathbf{a}_\lambda)_z|\phi_{\Lambda'}(E')>\Big]\,, \end{aligned} \tag{11}$$

with $\mathbf{a}_\lambda$ being a polarisation vector and $\mathbf{B} = B\,\hat{\mathbf{z}}$ has been assumed.

The above scheme has recently been applied for the first time to the *fcc*-alloy system Fe_xNi_{1-x} [6]. This system was chosen because it possesses one of the highest SMA and is therefore of considerable technological importance. As Fig. 1 shows, the calculations reproduce satisfactorily the variation of the SMA with concentration. The most important reason for the much higher theoretical values compared with experiment seems to be the fact that the calculated isotropic resistivity $\bar{\rho}$ (not shown here) is to the same extent smaller than the experimental one. This is not unexpected because our calculations account only for the contribution to $\bar{\rho}$ due to scattering events caused by chemical disorder; any other sources such as e.g. short range order or grain boundaries are ignored.

In addition one should note that the calculations have been performed for $\hat{\mathbf{M}}[001]$ while the experimental data are for polycrystaline samples. However, as can be seen from measurements on single crystals, this contributes only neglegiblely to the deviation in Fig. 1.

In Fig. 1 results for the AHR are given in terms of the so-called Hall angle $\rho_H/\bar{\rho}$. Obviously, the agreement with experiment is comparable with that in the case of the SMA.

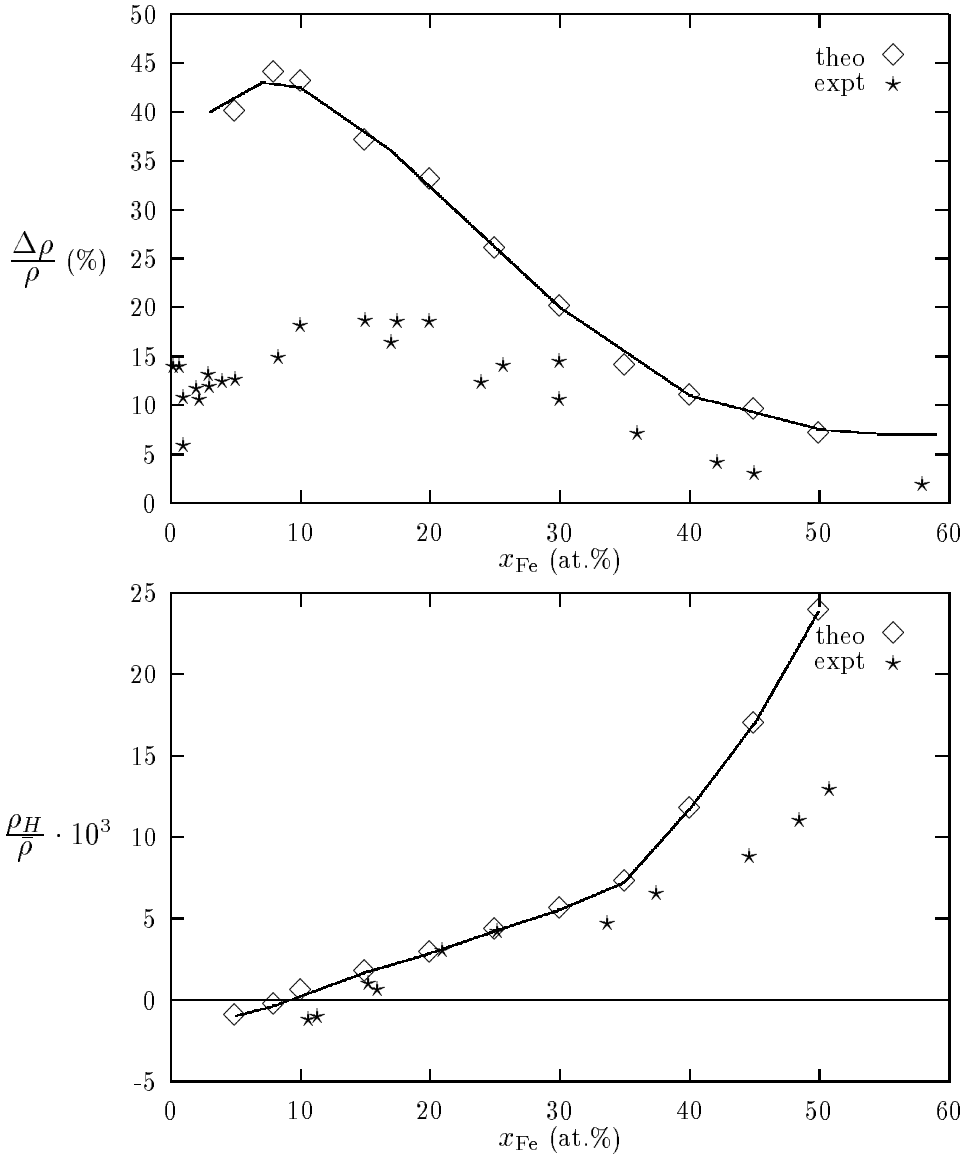

Figure 1: **Top:** Spontanous magneto-resistance anisotropy (SMA) $(\rho_{||} - \rho_{\perp})/\bar{\rho}$ of the disordered alloy system fcc-Fe_xNi_{1-x} for $T = 0K$. **Bottom:** Anomalous Hall resistivity (AHR) of fcc-Fe_xNi_{1-x} expressed by the Hall angle $\rho_H/\bar{\rho}$.

These calculations allowed to study the validity of various assumptions made within previous simple models for the SMA and AHR. For example, it turned out that calculating the SMA based on spin-resolved density of states at the Fermi energy together with a global parameter representing spin-orbit coupling is of rather limited usefullness. A test of the so-called two-current model common to all previous approaches is performed next. Evaluating the relevant matrix elements in the $\boldsymbol{\nabla}$-form (see Eq. (10)) it was found that the additional terms that allow for spin-flip scattering events are by a factor of 100 smaller than the $\boldsymbol{\nabla}$-related part. This means that hybridisation of states with different spin character due to spin-orbit coupling is by far the most important source for the SMA and AHR.

Finally, one should emphasize that the results presented here clearly demonstrate that the

spin only Hamiltonian in Eq. (1) contains all the relevant physics to allow for a proper description of the SMA and AHR.

6 Magneto-optical Kerr-effect

Any material with a non-diagonal conductivity tensor $\boldsymbol{\sigma}(\omega)$ will in general turn incoming linearly polarised light into elliptically polarized one. If this property of $\boldsymbol{\sigma}(\omega)$ is – at least partly – due to the magnetisation then the effect observed in reflection is called magneto-optical Kerr-effect. The complex Kerr-angle $\phi_K = \theta_K + i\epsilon_K$ combines the Kerr-rotation angle θ_K of the polarisation ellipsis, with respect to the original polarisation vector, and its ellipticity ϵ_K. For a system with at least 3-fold symmetry (i.e. trigonal, hexagonal, tetragonal and cubic) and the magnetisation as well as the incoming beam along the surface normal $\hat{\mathbf{z}}$ (polar geometry) the complex Kerr-angle ϕ_K is given by:

$$\phi_K = \frac{-\sigma_{xy}}{\sigma_{xx}\sqrt{1 + i\left(\frac{4\pi}{\omega}\right)\sigma_{xx}}} \,. \tag{12}$$

In principle the version of the Kubo-Greenwood-equation (8) for finite frequencies could be used in a straightforward way to calculate $\boldsymbol{\sigma}(\omega)$ and from that $\phi_K(\omega)$. Alternatively, one can calculate the absorptive parts of σ_{xx} and σ_{xy} using the expressions:

$$\sigma_{xx}^{(1)} = \frac{\pi e}{2\hbar\omega m V} \sum_{\substack{n\,\mathbf{k}\,\text{occupied} \\ n'\,\mathbf{k}\,\text{unoccupied}}} \left[|< n'\mathbf{k}|\, j_- \,|n\mathbf{k}>|^2 + |< n'\mathbf{k}|\, j_+ \,|n\mathbf{k}>|^2 \right] \delta(\omega_{nn'} - \omega) \tag{13}$$

$$\sigma_{xy}^{(2)} = \frac{\pi e}{2\hbar\omega m V} \sum_{\substack{n\,\mathbf{k}\,\text{occupied} \\ n'\,\mathbf{k}\,\text{unoccupied}}} \left[|< n'\mathbf{k}|\, j_- \,|n\mathbf{k}>|^2 - |< n'\mathbf{k}|\, j_+ \,|n\mathbf{k}>|^2 \right] \delta(\omega_{nn'} - \omega) \tag{14}$$

and determine the corresponding dispersive parts by a Kramers-Kronig transformation. With $j_\pm = j_x \pm i j_y$ Eqs. (13) and (14) emphasize that $\sigma_{xx}^{(1)}$ and $\sigma_{xy}^{(2)}$ can be viewed respectively as the average and difference of the absorption coefficients for the left and right circularly polarized light.

The expressions in Eqs. (13) and (14) represent only contributions due to $\mathbf{k}$-conserving inter-band transitions ($n \neq n'$). The intraband transitions are conventionally taken into account in a phenomenological way by the so-called Drude term. Fortunately, this contribution to $\boldsymbol{\sigma}$ can safely be neglected for $\omega \gtrsim 1.5 - 2$ eV.

The form of $\boldsymbol{\sigma}$ given in Eqs. (4) and (5) expresses the fact that changing the orientation of $\mathbf{M}$ from [001] to [110] the true symmetry of the system changes from tetragonal to orthorhombic. From this one can expect a corresponding anisotropy for the Kerr spectra $\theta_K(\omega)$. As can be seen in Fig. 2 this anisotropy is found to be completely neglegible for fcc-Co [7]. This finding is in full agreement with the experimental data of Weller et al. [8] for Co-films with [001]- and [110]-orientation. Obviously, spin-orbit coupling in fcc-Co is responsible for the Kerr-effect

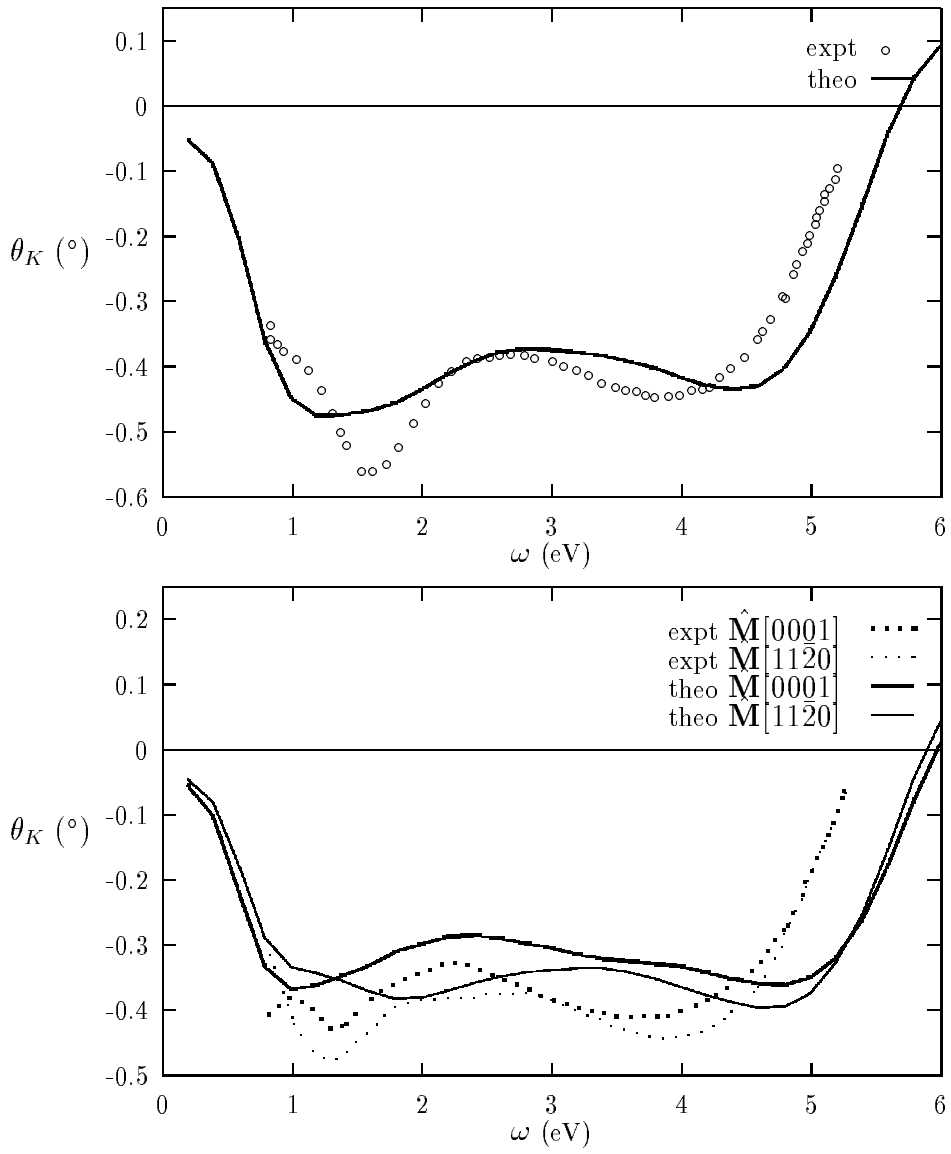

Figure 2: **Top:** Kerr-rotation angle θ_K for fcc-Co with $\hat{\mathbf{M}}[001]$ and $\hat{\mathbf{M}}[110]$. The theoretical spectra for both orientations practically coincide. For the experimental curves only small differences have been found. **Bottom:** Kerr-rotation angle θ_K for hcp-Co with $\hat{\mathbf{M}}[0001]$ and $\hat{\mathbf{M}}[11\bar{2}0]$.

but it is too weak to produce any significant anisotropy for $\theta_K(\omega)$. This situation is similar to the spin-orbit induced field gradient in cubic magnetic solids. This phenomenon, like the Kerr-effect, is a direct manifestation of the reduced symmetry compared to the paramagnetic state. However, even for 5d-elements in an Fe-matrix no significant anisotropy for the field gradient could be detected so far. For hcp-Co the situation completely differs from that for fcc-Co. Here, because of the crystal structure the optical properties are anisotropic even for the paramagnetic state. Thus the anisotropy induced by the magnetic state is superimposed onto that due to the crystal structure. For this reason, in contrast to fcc-Co, there is a clear anisotropy present as can be seen in Fig. 2. Again the experimental data were obtained by

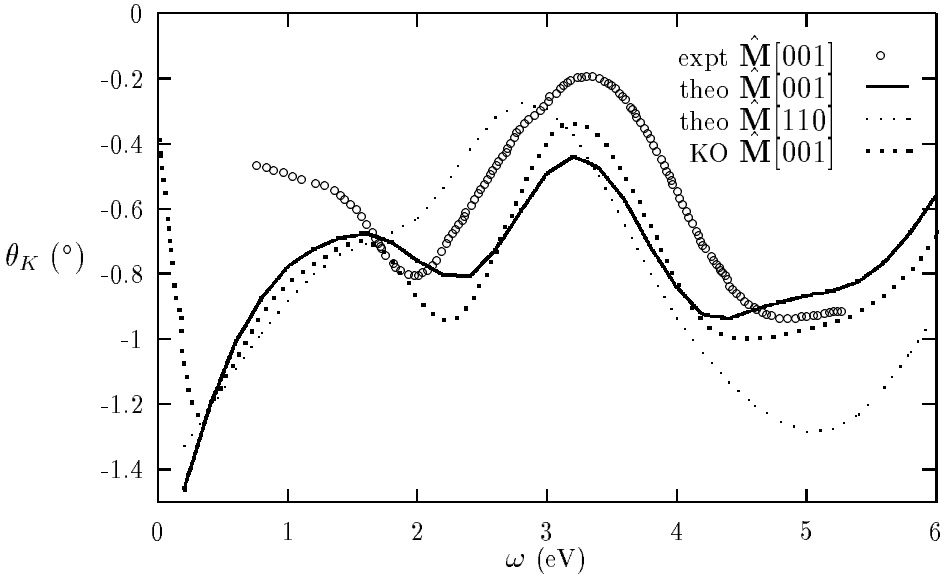

Figure 3: Kerr-rotation angle θ_K for FePt for various orientations. KO stands for Kübler, Oppeneer et al.

Weller et al. for films with [0001]- and [11$\bar{2}$0]-orientation. In line with the anisotropy of θ_K an anisotropy for the total magnetic moment and the hyperfine fields is found (0.004 μ_B and 5.7 kG compared to the experimental values 0.008 μ_B and 8 kG, respectively). In both cases the anisotropy is due to their orbital parts which occur – like θ_K – due to the spin-orbit coupling. However, θ_K gives more detailed (at least partly) energy resolved information on the anisotropy while the orbital moments and hyperfine fields are integral properties of the occupied states.

The hcp-Co could be viewed as a simple layered structure system. For this reason one can expect that the anisotropy of θ_K is more pronounced for a true layered structure, e.g., for the compound FePt in the CuAu-structure. This indeed can be seen from the theoretical spectra in Fig. 3 [9]. Remembering the role of the Drude contribution for $\omega \lesssim 1-2$ eV our results for the [001]-orientation are in fairly good agreement with the experimental results of Weller et al. It seems that so far the preparation of the corresponding films for the [110]-orientation has not been successful. In Fig. 3 we have included the theoretical results of Kübler, Oppeneer et al. [10]. This group is using the scalar-relativistic ASW and accounting for spin-orbit coupling in the variational step, while the results presented so far were obtained using the SPRLMTO-ASA. Because the spectra agree as far as one might expect for two completely different calculations (using presumably slightly different atomic radii, lattice constants and lifetime parameters) one can conclude that: i) for calculating Kerr-spectra and other spin-orbit induced properties it is in general not necessary to use the approach based on the Dirac equation (see Eq. (1)) – even for systems containing heavy elements like Pt, ii) because in the ASW-calculations of Fig. 3 the interstitial region is treated more accurately it is obvious that evaluating the matrix elements of $\mathbf{j}$ in the $\boldsymbol{\nabla}$-form essentially

cure the problems with the $\boldsymbol{\alpha}$-form.

Furthermore, using Eq. (10) it was found – as before for $\boldsymbol{\sigma}(\omega = 0)$ of Fe_xNi_{1-x} – that spin-flip transitions play only a minor role ($\approx$ 1%). Thus the estimate ($\approx$ 10%) often found in the literature seems to be unrealistic.

Finally, it should be emphasized that statement i) does not mean that the Hamiltonian in Eq. (1) does not have any advantages compared to the variational treatment of spin-orbit coupling. For example treating alloy systems within the CPA would be quite cumbersome using the latter approach. Furthermore future developments in relativistic density functional theory will presumably provide a natural extension of the Hamiltonian in Eq. (1).

7 Magnetic X-ray dichroism

In recent years various experimental groups have demonstrated that the magneto-optical Kerr effect (MOKE) can also be observed in the X-ray regime. This means that although the nature of the initial states completly changes – tightly bound core states versus the itinerant valence band states for the optical regime – the physics remains the same. Much easier than observing the MOKE in the X–ray regime is however the corresponding absorption experiment. For a discussion of that experiment it is obviously sufficient to look at the absorptive parts of the elements of $\boldsymbol{\sigma}$. From the form of $\boldsymbol{\sigma}$ in Eq. (4) one can easily see that different kinds of dichroism i.e. dependencies of the absorption on the polarisation of the radiation may occur. The occurence of σ_{xy} gives rise to the circular dichroism meaning that the absorption coefficients for left and right circularly polarized X–rays, μ_+ and μ_-, respectively, are different. From Eq. (13) and (14) one easily sees that $\mu_\pm \propto \sigma^{(1)}_{xx} \pm \sigma^{(2)}_{xy}$. The difference between σ_{xx} and σ_{zz}, giving rise to the SMA for $\omega = 0$, leads to a linear dichroism, i.e. to different absorption coefficients μ_λ for X–ray linearly polarized parallel to $\hat{\mathbf{M}}$ ($\mu_\parallel \propto \sigma^{(1)}_{zz}$) and perpendicular to $\hat{\mathbf{M}}$ ($\mu_\perp \propto \sigma^{(1)}_{xx}$). Eqs. (4) and (5) also demonstrate that one can have different kinds of linear dichroism. The one just described occurs if $\hat{\mathbf{M}}$ is fixed and the polarisation vector is changing. But there is another one for the polarisation fixed and the magnetisation rotated, because for example $\sigma^{(1)}_{zz}(\hat{\mathbf{M}}\ [001])$ may differ from $\sigma^{(1)}_{zz}(\hat{\mathbf{M}}\ [110])$.

A very flexible scheme to calculate the absorption coefficient μ_λ was developed some years ago based on the SPRKKR-method. Alternatively, one can also use the SPRLMTO-method to calculate μ_λ in analogy to Eqs. (13) and (14) from

$$\mu_\lambda \propto \sum_{\substack{i \text{ occupied} \\ n\,\mathbf{k} \text{ unoccupied}}} |< n\mathbf{k}|\, j_-\, |i>|^2\, \delta(\omega_{ni} - \omega). \tag{15}$$

As stated above only the nature of the initial state has changed from a Bloch state $|n\mathbf{k}>$ to a core state $|i>$. This has the important consequence that the resulting spectra are not

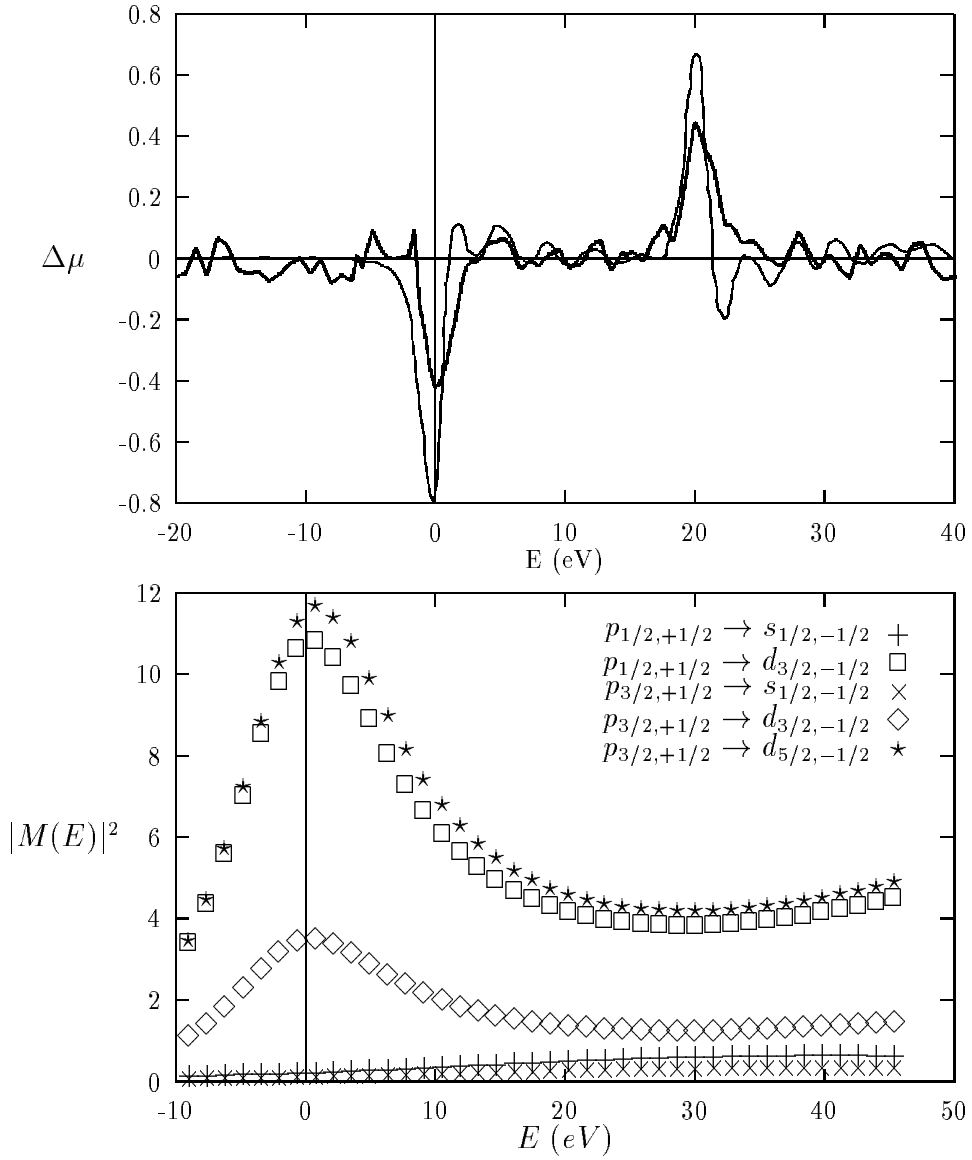

Figure 4: **Top:** Circular dichroism $\Delta\mu = \mu^- - \mu^+$ at the $L_{2,3}$-edge of Cu in the multilayer system Co5/Cu4. Theory: full line, experiment: dashed line. **Bottom:** Matrix elements for the various $2p_{j,\mu} \rightarrow 4s(3d)_{j,\mu'}$-transitions with $\mu = +1/2$ and $\mu' = -1/2$ at the $L_{2,3}$-edge of Cu.

anymore linked to the so-called joint density of states but just to the density of unoccupied states. As a result, the interpretation of the resulting spectra is tremendously simplified. Furthermore, again due to the nature of the initial state, the MXD provides a component specific probe of magnetism. This property has been used during the last years for a rapidly increasing number of studies on diluted and concentrated alloys as well as multilayer systems. As an example for such investigations Fig. 4 shows the circular dichroism at the $L_{2,3}$-edge of Cu in the multilayer system Co5/Cu4. Here the difference $\Delta\mu$ of the absorption coefficients for left and right circularly polarized radiation, μ^- and μ^+, resp., has been used as a measure for the dichroism, with the step at the absorption edge normalized to 100. Although the

dichroism signal is quite small (of the order of 1 %), it nevertheless reflects the polarisation of the Cu d-band states by the adjacent Co-layers. In most cases $\Delta\mu$ can be viewed as an energy-resolved probe for the spin-polarisation of the final states. From the same sign of $\Delta\mu$ for Cu and Co (not shown here) in Co5/Cu4 one can therefore conclude that the Cu- and Co-moments are aligned in parallel – in accordance with the results of the bandstructure calculation. Using so-called sum rules (see references in [11]), which supply a basis for the above interpretation, a spin magnetic moment of around $0.014\mu_B$ could be deduced from the experimental spectra for Cu. This is in good agreement with the theoretical result ($0.0137\mu_B$). However, one has to keep in mind that one only gets an average value that way. For Co5/Cu4 this means an average for the two inequivalent Cu-layers. In more complex situations as for example Co2/Pt7 one has more inequivalent layers and may encounter corresponding partial spectra with different sign.

The reliability of the sum rules to deduce spin as well as orbital moments from MXD-spectra has recently been investigated in detail [11]. Comparing calculated moments of multilayer systems with moments deduced from corresponding MXD-spectra using the sum rules differences up to 40 % were found. For the orbital moment, for which the application of the sum rules is somewhat simpler, the ratio of the calculated and deduced values was found to be close to 0.67 in all cases.

Although the sum rules applied to experimental spectra gave so far reasonable estimates for the spin and orbital moments in a great variety of systems one should emphasize that these estimates strongly depend on the filtering of the MXD-spectra from the raw data i.e. on the background subtraction. On the other hand one should also emphasize that one of the basic assumptions in deriving the sum rules, namely energy independent radial matrix elements, is rarely fulfilled. Fig. 4 shows corresponding data for the $L_{2,3}$-edge of Cu. As one can see the most important matrix elements vary nearly by 50 % in the energy range $(E - E_F) = 0 - 10eV$. In addition one finds that the $p \rightarrow d$-matrix elements are much larger than those of the $p \rightarrow s$-transitions. This is, of course, primarily caused by the fact that the relevant $2p-$ and $3d-$radial wavefunctions are nodeless while the $4s-$function has three nodes. As a consequence of this the MXD-spectrum in Fig. 4 is dominated by $p \rightarrow d$-transitions although for Cu the $s-$, $p-$ and $d-$densities of states above the Fermi level are of the same order of magnitude.

8 Concluding remarks

The linear response conductivity tensor $\boldsymbol{\sigma}(\omega)$ has been used to demonstrate close relations between various phenomena which at first sight seem to be quite different in nature. Considering the symmetry properties of $\boldsymbol{\sigma}(\omega)$ it becomes obvious that it is spin-orbit coupling together with spin-polarisation that gives rise to the spontanous magnetoresistance anisotropy, the anomalous Hall resistivity, the magneto-optical Kerr-effect, the magnetic X-ray dichroism

and so on. Of course dealing with spectroscopies that are influenced by surface properties — as for example the spin- and angle-resolved UPS — the situation may be more complicated and the symmetry considerations may have to be extended accordingly.

The examples presented here demonstrate that used here spin-only Dirac-Hamiltonian provides a firm basis for a theoretical investigation of the various spin-orbit induced phenomena in magnetic solids. However, there are also clear indications coming primarily from MXD-spectroscopy of shortcomings to this approach. These might be linked to the observation that the calculated orbital moments in general turn out to be too small. Obviously further work in that direction needs to be done.

References

[1] A. H. MacDonald and S. H. Vosko J. Phys. C: Solid State Phys. **12**, 2977 (1979).

[2] R. Feder and F. Rosicky and B. Ackermann, Z. Physik B **52**, 31 (1983).

[3] P. Strange and J. B. Staunton and B. L. Gyorffy J. Phys. C: Solid State Phys. **17**, 3355 (1984).

[4] W. H. Kleiner, Phys. Rev. **142**, 318 (1966).

[5] W. H. Butler, Phys. Rev. **B31**, 3260, (1985).

[6] J. Banhart and H. Ebert, submitted.

[7] G.-Y. Guo and H. Ebert, Phys. Rev. **B50**, 10377, (1994).

[8] D. Weller, G. R. Harp, R. F. C. Farrow, A. Cebollada, and J. Sticht, Phys. Rev. Lett. **72**, 2097, (1994).

[9] G.-Y. Guo and H. Ebert, Phys. Rev. **B**, submitted.

[10] I. Osterloh, P. M. Oppeneer, J. Sticht, and J. Kübler, J. Jhys. Condens. Matter **6**, 285, (1994).

[11] G.-Y. Guo, H. Ebert, W. M. Temmerman, and P. J. Durham, Phys. Rev. **B50**, 3861, (1994).

[12] *a more complete list of references can be found in the references given above*